JOURNAL OF WATER AND LAND DEVELOPMENT
e-ISSN 2083-4535

Polish Academy of Sciences (PAN), Committee on Agronomic Sciences
Institute of Technology and Life Sciences (ITP)

JOURNAL OF WATER AND LAND DEVELOPMENT
2021, No. 49 (IV–VI): 244–251; https://doi.org/10.24425/jwld.2021.137118

Available (PDF): https://www.itp.edu.pl/JWLD; http://journals.pan.pl/jwld

Received 16.09.2020
Reviewed 03.12.2020
Accepted 29.12.2020

Flow characteristics after installation of floating bridge in open channel

Mohamed M. IBRAHIM[1)], Mahmoud A.R. ELTOUKHY[1)], Adnan D. GHANIM[2)]

[1)] Benha University, Shoubra Faculty of Engineering, PO Box 11629, Shoubra, Egypt
[2)] Advisor to the President of the Iraqi Council of Representatives, Iraq

For citation: Ibrahim M.M., Eltoukhy M.A.R., Ghanim A.D. 2021. Flow characteristics after installation of floating bridge in open channel. Journal of Water and Land Development. No. 49 (IV–VI) p. 244–251. DOI 10.24425/jwld.2021.137118.

Abstract

A pontoon bridge, also known as a floating bridge, can be used as for pedestrian and vehicle traffic. The buoyancy of the floating bridge limits the maximum load it can carry. This research included experimental runs to study variations of open channel flow characteristics upstream and downstream a floating bridge. Eighty one runs have been carried out using a flume in a hydraulic laboratory. The experimental run program is classified into two main categories; the first investigates the velocity ratios (v_{ds}/v_{us}) downstream and upstream the floating bridge. The second category is concerned with the energy head losses (h_L) due to the presence of a floating bridge. The experimental runs are carried out using three pontoon lengths, three flow depths, six submerged depths, and three discharges. The results are analysed and graphically presented to help predict hydraulic parameters. The outcomes have shown that the floating bridge upstream, Froude number and submergence of the pontoon are the dominant parameters that affect the studied flow characteristics.

Key words: *floating bridges, flow characteristics, flume, head loss, velocity*

INTRODUCTION

Floating bridges can be permanent or temporary and supported by pontoons. Most pontoon bridges are temporary, used in wartime and civil emergencies. Permanent floating bridges are useful for sheltered water-crossings where it is not considered economically feasible to suspend a bridge from anchored piers. Photo 1 shows an example for a floating bridge and its support a continuous deck for vehicle and pedestrian travel. Floating bridges are easy and quickly constructed within an economic cost. Social benefits documented are substantial, as they improve the infrastructure between cities and other areas.

Such bridges require a section that is elevated, or can be raised or removed, to allow waterborne traffic to pass [FREDERIKSEN *et al*. 2019]. BREDE [2017] recognized that bridges are effective ways of connecting islands and peninsulas. VAN JOHNSON [2018] investigated floating bridges and stated that they may replace conventional bridges due to technical, practical, and economic reasons.

Photo 1. Typical example of a floating bridge (photo: https://www.mabeybridge.com/products/bridging/mabey-floating-bridge2)

On the one hand, most studies of floating bridges examine them from a mechanical point of view. SHIXIAO *et al*. [2005] performed a hydro-elastic analysis of a nonlinearly connected floating bridge associated with moving loads and provided an equation for its dynamic response. ABOZAID *et al*. [2016] studied the structural performance of hybrid composite floats in comparison with steel.

On the other hand, many researchers scrutinized floating bridges from the hydraulic or hydrodynamic points of view. One of the most common topics in the hydraulic study of floating bridges are velocity distributions and energy head losses. They are considered to be essential parameters causing bed scouring which effectively changes the canal bed morphology [ARNESON *et al*. 2012]. The presence of a floating bridge affects the velocity distribution upstream, underneath, and downstream, and also the energy head loss, which are considered important parameters in the design process. The floating bridge sensitivity depends on its components and the bridge may become more susceptible to spatially altered excitations [MA *et al*. 2019]. Energy head loss occurs when the water body flows through the bridge [WANG *et al*. 2019].

WEHAUSEN and LAITONE [1960] studied the open channel flow in presence of a floating bridge. Books on hydrodynamic should be consulted, as they provide an explanation of the interaction of a fluid structure. Moreover, NEWMAN [1977] indicated the importance of studying hydrodynamics, as it provided general information on hydrodynamics, describe water waves as they interact with the installed structures, treated various problems of fluid movement, described wave motion and dealt with various hydrodynamic problems. HELAL *et al*. [2018] carried out two hundred and twenty nine experimental runs to study the bed morphology in an open channel due to presence of a floating bridge. They also investigated the energy head loss on a static floating bridge with constant and variable submergence ratios. They deduced empirical equations for scour parameters, predictions, and flow characteristics. The results indicated that Froude number and floating bridge submergence dominate regarding the impact on bed morphology and flow characteristics. ETTEMA *et al*. [2006] investigated the major floods in the Midwest in several consecutive decades. They determined that flash floods occur frequently on an annual basis and they affect small bridges in Iow.

Some studies scrutinized floating bridges from the structural point of view. SEIF and INOUE [1998] analysed floating bridges subjected to wave loading by varying the contributing parameters. PETERSEN *et al*. [2019] studied the dynamic behaviour of long-span bridges under stochastic loads from typically ambient excitation sources. In real life, these loads cannot be measured directly at a full scale. DENG *et al*. [2018] reported that the wave attenuation is frequency--dependent and effective for the common wave frequencies. KOU *et al*. [2019] applied numerical model based on the potential flow theory and finite element method (FEM) to predict the wave-induced hydro-elastic responses of flexible floating bridges.

This research included experiments and investigations of floating bridges and their impact on waterways. This was done by studying downstream to upstream velocity ratios and the resulting energy head loss due to the presence of floating bridges.

STUDY METHODS

EXPERIMENTAL SETUP

The flume used in the hydraulic laboratory is built on the ground and considered as a recirculating type. The model is a closed operating system with a 20 m overall length, 0.7 m wide and 0.5 m deep for allover the flume except 0.75 m deep for the study area of 4 m length. Water is supplied to the flume through the inlet pipe by means of five centrifugal pumps to supply three different discharges of 50, 70, and 110 $dm^3 \cdot s^{-1}$. Figure 1 and Photos 2 and 3 show the layout and photos for the flume. The model has a concrete bed and brick side walls, with brick dimensions

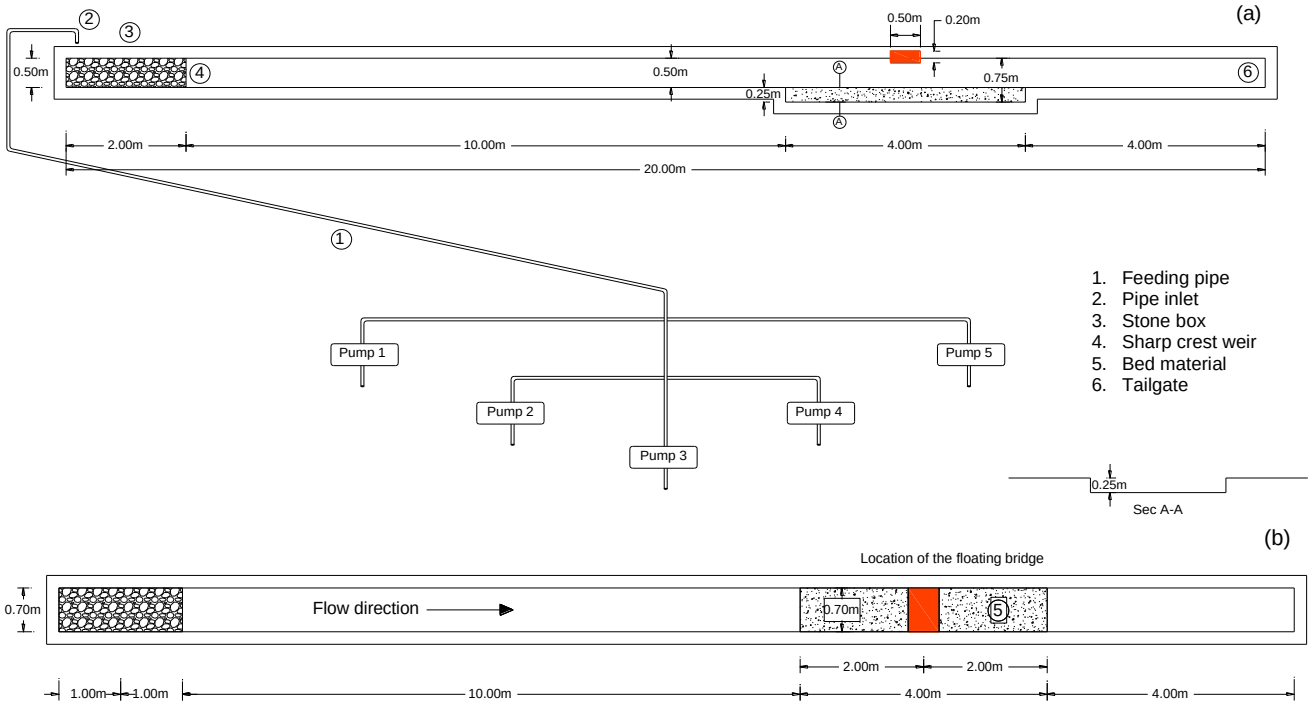

Fig. 1. The flume layout: a) elevation, b) plan; source: own elaboration

Photo 2. Photographic shots during the experimental setup (photo *A.D. Ghanim*)

Photo 3. The floating bridge model in the hydraulic laboratory (photo *A.D. Ghanim*)

of 20×20×40 cm. They are placed and plastered by cement mortar. A sharp crested weir of 70×35×0.4 cm is placed across the flume at its beginning to ensure discharge measurements by electromagnetic flowmeters. A steel caisson that covered 0.1*L* of the flume of 70×50×40 cm is filled with gravel in order to dissipate energy, regulate the flow over the weir, and to ensure that water has uniform flow in the flume. The floating bridge model is installed and accurately placed into the flume at its mid-section between 0.6*L* and 0.8*L* with the center of the floating bridge model exactly located at 0.7*L*, as shown in Figure 3. The channel bed is covered by 0.25 m soil of d_{50} = 0.48 mm. A steel tilted gate is located at the end of the flume to control water depth. Velocity is measured at depths of 0.2, 0.6, and 0.8 by mini flowmeter of its outer diameter 7.0 mm with the accuracy of ±2%. In addition, water levels are measured by a single point gauge.

EXPERIMENTAL PROGRAM

The experimental program has encompassed eighty one experimental runs summarized in Table 1. To simulate the different flow conditions in open channel, three discharges and three water depths are used. Regarding the floating bridge model, three lengths are investigated under different draft depths in order to determine the impact of the floating bridge on the downstream to upstream velocities ratios $v_{ds}/v_{us,}$ and the energy head loss. Figures 2 and 3 are presented to explore the flow pattern in the vicinity of the floating bridge, and the locations of velocity measurements for each bridge length. The measurements cover 4 m length of the experimental model and are distributed in six locations along the channel center line. Two measuring points are located upstream of the bridge model and the rest are down-

Table 1. Experimental runs program

Discharge Q ($dm^3 \cdot s^{-1}$)	Water depth y (cm)	Bridge length L_b (cm)	Bridge draft d (cm)
50	12	50	7, 9, 10.5
	14	60	6, 8, 9
	16	70	4, 6, 7
70	12	50	7, 9, 10.5
	14	60	6, 8, 9
	16	70	4, 6, 7
110	12	50	7, 9, 10.5
	14	60	6, 8, 9
	16	70	4, 6, 7

Source: own elaboration.

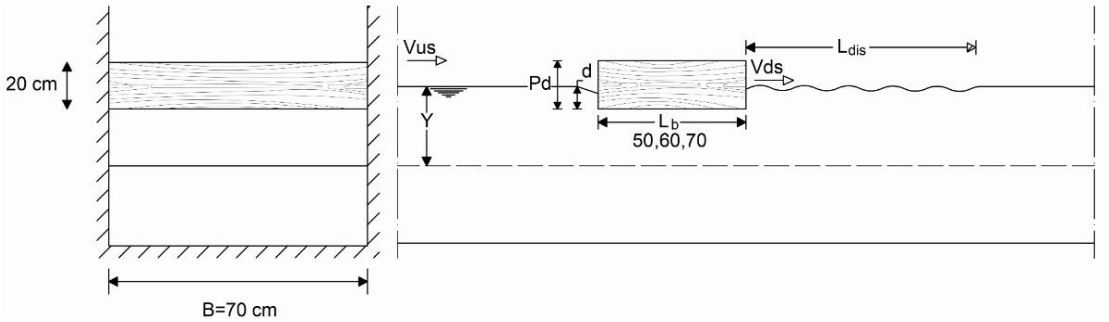

Fig. 2. Sketch for flow pattern at the location of floating bridge; v_{us} = velocity upstream, v_{ds} = velocity downstream, P_d = pontoon bridge depth, d = bridge draft (submerged depth), L_b = pontoon bridge length, L_{dis} = downstream disturbed length; source: own elaboration

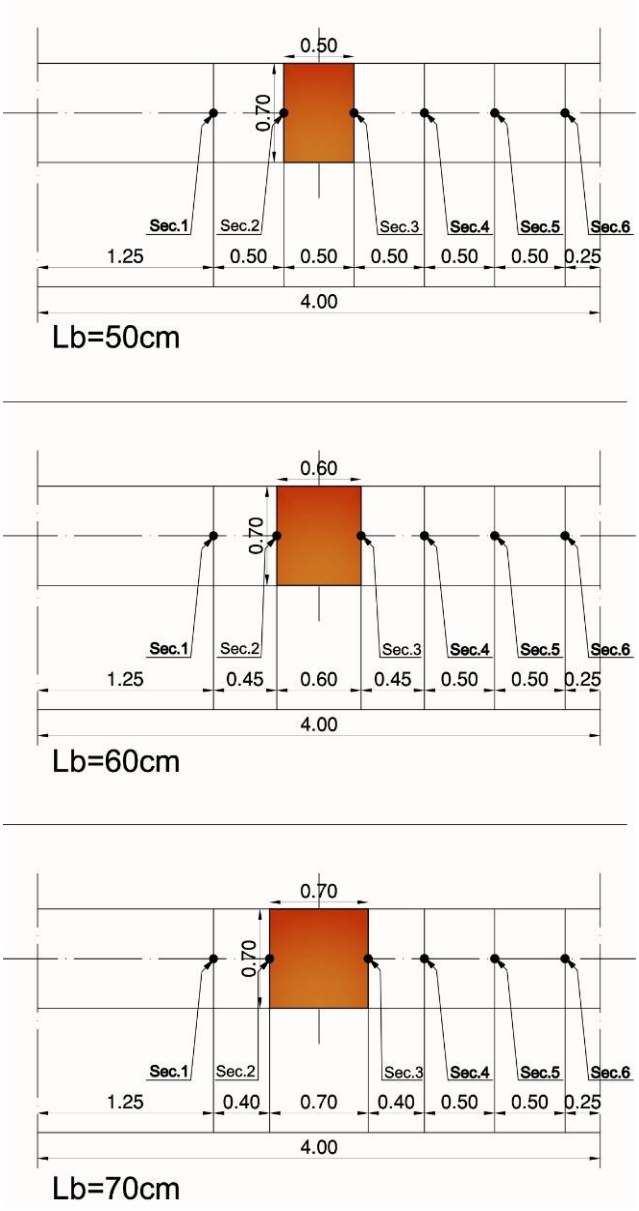

Fig. 3. Locations of velocity measurements, plan view; source: own elaboration

stream where the significant influence on the flow characteristics is expected to occur due the installation of the floating bridge.

RESULTS AND DISCUSSION

MODEL VALIDATION

Firstly, the flume results validation has been done by comparing the current experimental results with that concluded by previous studies displayed in the review section. The outcomes by HELAL *et al.* [2018], FREDERIKSEN *et al.* [2019], ABOZAID *et al.* [2016], and PETERSEN *et al.* [2019] are used for this purpose. The comparative results are presented in Figure 4. According to comparative investigations, it can be noted that the results are convergent with the present measurements, where around 80% of the data are within the ±21% error band and around 91% are within ±34% error band. Therefore, the experimental data are acceptable comparing to the data collected from the review.

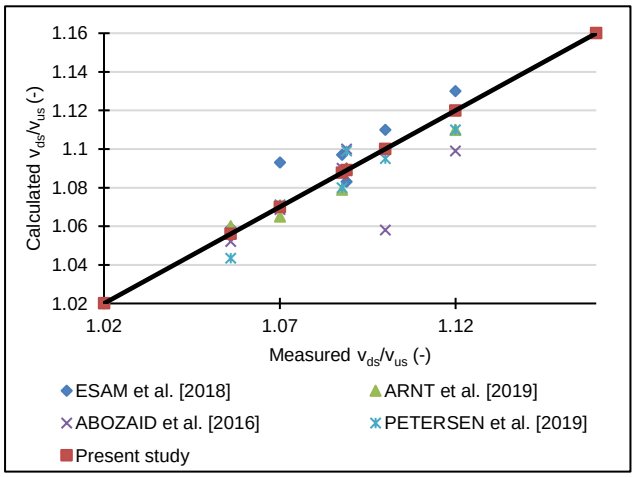

Fig. 4. Comparison between present and previous studies; v_{ds} = velocity in the downstream, v_{up} = velocity in the upstream; source: own elaborations

With respect to the flow characteristics, numerous parameters are affected because of the presence of the floating bridge. These include mainly the floating bridge downstream to upstream velocities ratio v_{ds}/v_{up} and energy head loss h_L. The parameters associated in this research are the floating bridge length L_b, pontoon bridge depth P_d, pontoon width P_w, bridge draft (submerged depth) d, flow discharge Q, mean flow velocity v, flow depth measured away from the floating bridge effect (2 m before the tail gate) y (Fig. 2 and Tab. 1).

The open channel flow characteristics and other parameters can be gathered based on the flow characteristics (g, v_{us}, v_{ds}, y, h_L, μ, ρ) and the floating bridge geometry (P_w, d, L_b, P_d). The dimensionless groups according to Buckingham π-theorem are as follows:

$$f(g, v_{us}, v_{ds}, y, h_L, \mu, \rho, P_w, d, L_b, P_d) \quad (1)$$

where: F_r = the upstream Froude number calculated at the section, where y is measured ($Fr = \frac{V}{\sqrt{g\,y}}$). The considered flow condition is turbulent, hence μ (dynamic viscosity of water) can be neglected. During the experimental runs, the gravitational acceleration g = 9.81 m·s^{-2}, pontoon width P_w = 70 cm, and the pontoon bridge depth P_d = 20 cm are constant. After some arrangements for Equation (1), it can be deduced that:

$$f\left(\frac{d}{y}, \frac{h_L}{y}, \mathrm{Fr}, \frac{P_d}{y}, \frac{v_{ds}}{v_{us}}\right) = 0 \quad (2)$$

$$\frac{v_{ds}}{v_{us}} = f\left(\frac{d}{y}, \mathrm{Fr}, \frac{P_d}{y}\right) \quad (3)$$

$$\frac{h_L}{y} = f\left(\frac{d}{y}, \mathrm{Fr}, \frac{P_d}{y}\right) \quad (4)$$

The measurements of experimental runs are recorded, analysed and graphically presented in charts. The analysis is presented into two main categories: the velocity ratio v_{ds}/v_{up} and the head loss h_L as per Equations (3) and (4), respectively.

FLOATING BRIDGE DOWNSTREAM TO UPSTREAM VELOCITIES RATIO

The first category of the experimental runs focuses on studying the variation of the floating bridge downstream to upstream velocities ratio, v_{ds}/v_{up}. The parameters regarding the analysis process are the discharge Q of 50, 70, and 70 dm^3·s^{-1} which measured with calibrated mini flowmeter; submergence ratio d/L_b of 0.14, 0.18, and 0.21 corresponding to L_b = 50 cm. Also, the floating bridge downstream to upstream velocities ratio v_{ds}/v_{up} and ratio results are analysed for different pontoon bridge L_b/P_d ratios of 2.5, 3.0, and 3.5.

Figure 5 is plotted to characterize the influence of upstream Froude number on v_{ds}/v_{up} for different values of d/L_b under various discharges. From the analysis of the outcomes, it can be seen that all measurements of v_{ds}/v_{up} in the presence of the floating bridge are greater than one. That implies the velocity downstream the floating bridge is greater than upstream. The figures additionally show that the floating bridge downstream to upstream velocity ratio v_{ds}/v_{up} increases as the Froude number increases regardless the discharge. Emphasizing the impact of the submergence ratio d/L_b, the figures show that for constant upstream Froude number, the v_{ds}/v_{up} increases as the submergence ratio, d/L_b increase. The reported findings are due to the contraction in the flow area created by the presence of the bridge model.

Figure 6 shows the relation between v_{ds}/v_{up} ratio and the upstream Froude number under different discharges. Based on the analysis, it is derived that for d/L_b of 0.18 and Q of

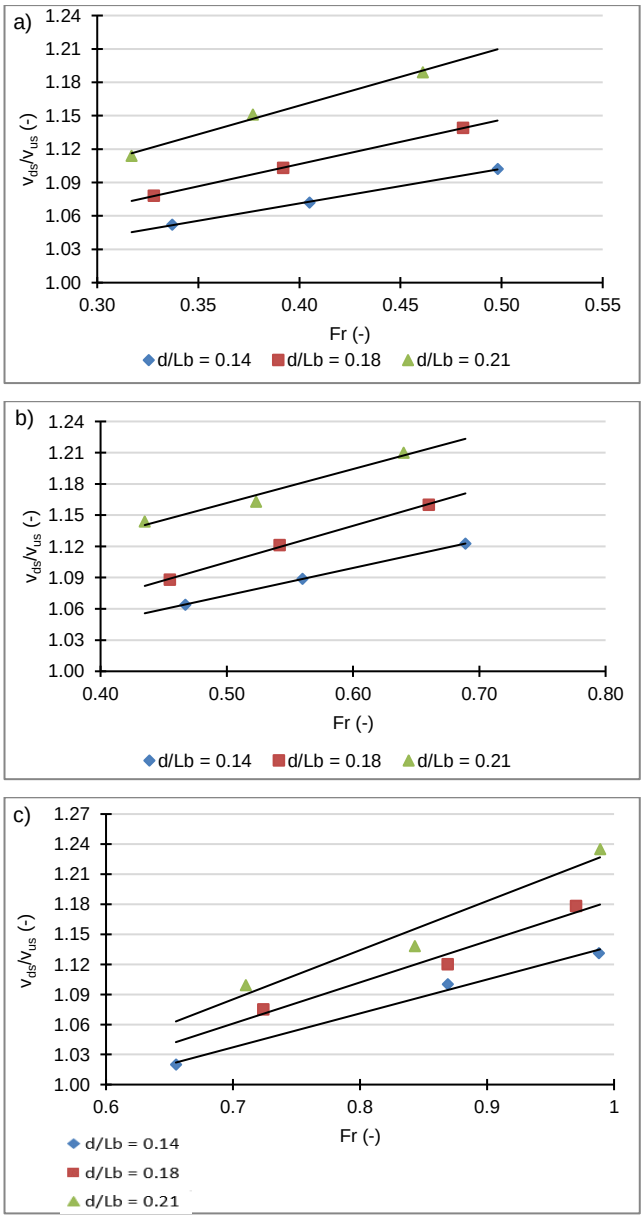

Fig. 5. Floating bridge downstream to upstream velocity ratio for flow discharge: a) Q = 50 dm^3·s^{-1}, b) Q = 70 dm^3·s^{-1}, c) Q = 110 dm^3·s^{-1}, d = bridge draft, L_b = pontoon bridge length; source: own study

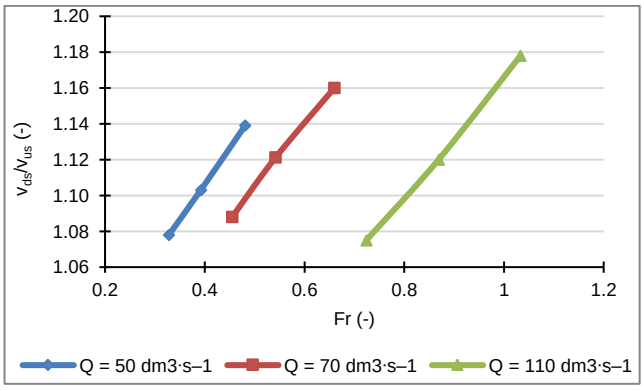

Fig. 6. Floating bridge downstream to upstream velocity ratio v_{ds}/v_{up} for d/L_b = 0.18; d, L_b as in Fig. 5; source: own study

50 dm^3·s^{-1} the increase in the Froude number from 0.328 to 0.481 results in the increase of v_{ds}/v_{up} from 1.078 to 1.139. In other words, 46.65% increase in the Froude number leads to 5.66% increase in v_{ds}/v_{up}. Additionally, for the Froude number of 0.5 and d/L_b of 0.18, it has been found that the increase of the flow discharge Q by 40% results in the increase of v_{ds}/v_{up} by 1.8%. Finally, for Q of 70 dm^{3}s^{-1} and Froude number of 0.5, the v_{ds}/v_{up} increases by 8.4% as a result of 50% increase in the submergence ratio, d/L_b.

Figure 7 presents the impact of the upstream Froude number on v_{ds}/v_{up} for various values of d/P_d under L_b/P_d of 2.5, 3.0, and 3.5, respectively. The figures show the same results as discussed for the impact of the Froude number and submergence ratio on v_{ds}/v_{up} on the same pontoon bridge length ratio L_b/P_d. Additionally, for Froude number of 0.5 and d/P_d of 0.4, the increase in the pontoon bridge length ratio L_b/P_d from 2.5 to 3.5 prompts a decrease in v_{ds}/v_{up} from 1.12 to 1.06. This implies a 40% increase in L_b/P_d which results in 5.07% decrease in v_{ds}/v_{up}. It demonstrates that the velocity loss due to the presence of the floating bridge is proportional to the pontoon bridge length.

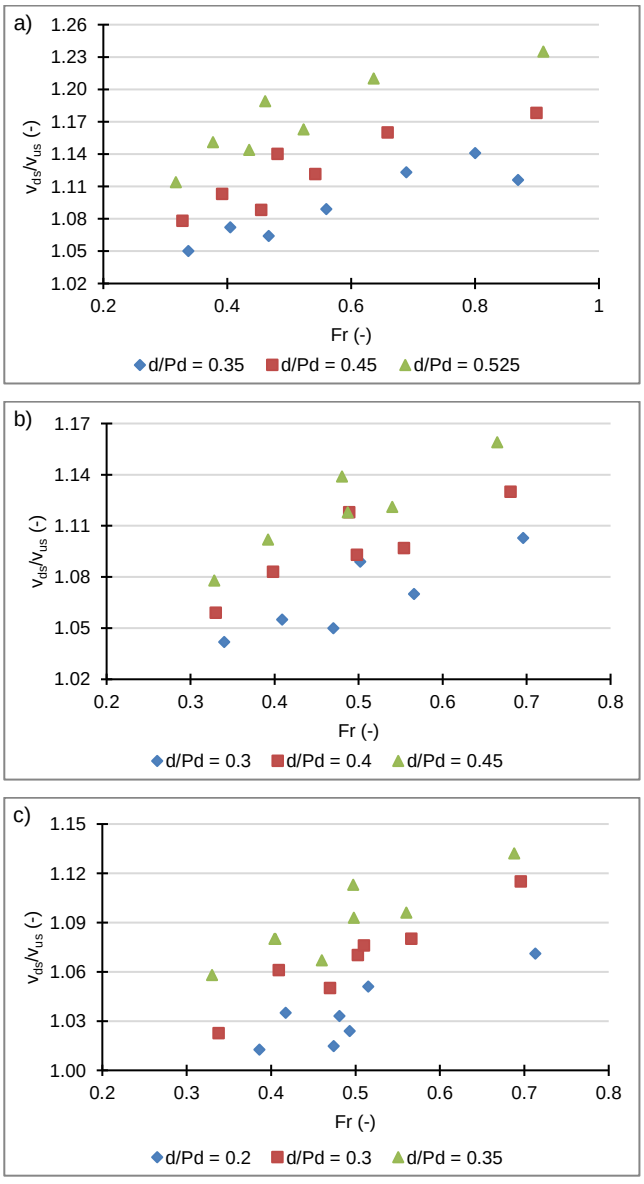

Fig. 7. Floating bridge downstream to upstream velocity ratio v_{ds}/v_{up} for: a) L_b/P_d = 2.5, b) L_b/P_d = 3.0, c) L_b/P_d = 3.5; L_b = pontoon bridge length, P_d = pontoon bridge depth; source: own study

Figure 8 has been introduced to explore the influence of d/y on v_{ds}/v_{up} for different pontoon bridge length ratio, L_b/P_d of 2.5, 3.0, and 3.5. The figure shows that the increase in d/y values demonstrates a recognizable increase in values of v_{ds}/v_{up} regardless the pontoon length ratio L_b/P_d.

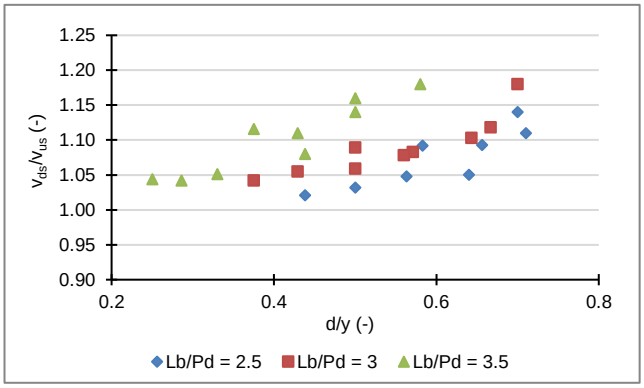

Fig. 8. Relationship between downstream and upstream velocity ratio v_{ds}/v_{us} and bridge draft to flow depht d/y for different values of L_b/P_d; L_b, P_d as in Fig. 7; source: own study

ENERGY HEAD LOSS IN PRESENCE OF FLOATING BRIDGE

In this sub-section, the second group of the experimental runs has been used to analyse parameters detailed in Equation (4) regarding the energy head loss due to the presence of the floating bridge. The energy head loss is calculated as follow:

$$h_L = E_{us} - E_{ds} = \left(y_{us} + \frac{v_{us}^2}{2g}\right) - \left(y_{ds} + \frac{v_{ds}^2}{2g}\right) \quad (5)$$

where: E_{us} = upstream energy, E_{ds} = downstream energy.

To examine the impact of Froude number on the energy head loss under different conditions of floating bridge emphasizing on d/P_d, and L_b/P_d ratios Figure 9 is introduced.

For any flow condition and characteristics of the bridge model, the figures show that the increase in the upstream Froude number Fr results in an increase in energy head loss h_L/y. Thus, the increase in Fr values leads to progressive increase in the flow velocity and consequently the increase in the head loss ratio h_L/P_d for constant P_d. Additionally, the increase in the submergence ratio d/P_d leads to an increase in values of h_L/y. Once the submergence ratio increases, the contracted area increases as well, which creates higher velocities, and increases the head loss.

According to Figure 10, it is deduced that the increase in d/y results in the increase in h_L/y. Moreover, the increase in d/y values results in an increase in the contracted area, which prompts higher velocity and increases the head loss ratio h_L/y. The figure also shows that the pontoon length has a significant influence on the energy head loss. The increase

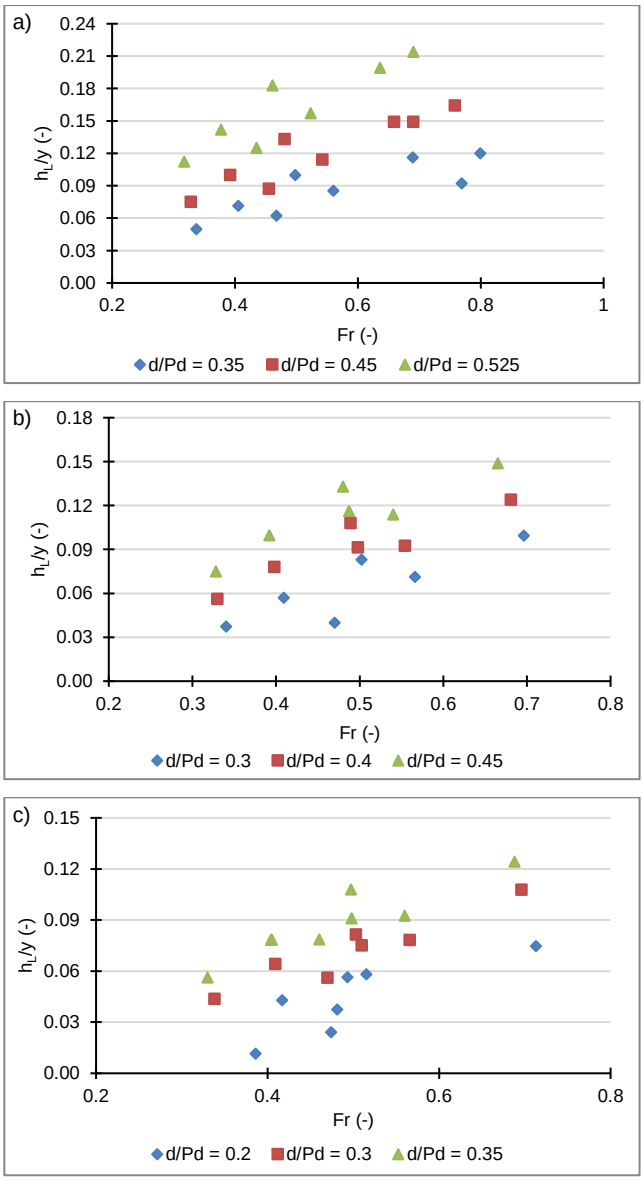

Fig. 9. Relationship between energy head loss h_L/y and Fr for different values of d/P_d, and ratio: a) L_b/P_d = 2.5, b) L_b/P_d = 3.0, c) L_b/P_d = 3.5; h_L = energy head loss, d = bridge draft, L_b, P_d as in Fig. 7; source: own study

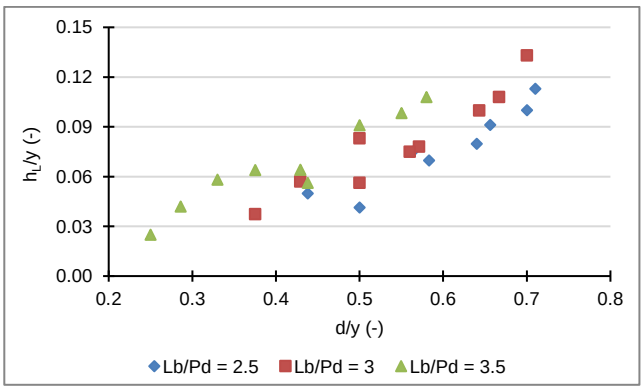

Fig. 10. Relationship between h_L/y and d/y for different values of L_b/P_d; hL = energy head loss, y = flow depth, d = bridge draft, L_b, P_d as in Fig. 7; source: own study

in the pontoon bridge length ratio L_b/P_d produces the increase in the energy head loss ratio h_L/y.

CONCLUSIONS

On the basis of the analysis of the obtained results of this experimental research, the following is concluded:

1. The use of a floating bridge affects the velocity distribution upstream, below, and downstream.
2. The floating bridge downstream to upstream velocity ratio v_{ds}/v_{up} increases with the increase of flow discharge which results in the increase in the Froude number and the increase in submergence ratios d/P_d.
3. The floating bridge downstream to upstream velocity ratio v_{ds}/v_{up} decreases with the increase of the pontoon bridge length L_b/P_d.
4. The increase in the flow discharge and hence Froude number results in the increase in energy head loss h_L/y.
5. Energy head loss h_L/y increases as the submergence ratio d/P_d increases.
6. As the pontoon bridge length ratio L_b/P_d increases, the energy head loss h_L/y decreases.
7. For future works, it is recommended that wide ranges of variables should be investigated together with numerical simulations to verify their results that can be collated with experimental and field data.

Notations

B = flume width (cm)
d = bridge draft (submerged depth) (cm)
E_{up} = upstream energy (m)
E_{ds} = downstream energy (m)
Fr = upstream Froude number (–)
g = gravitational acceleration (m·s^{-2})
h_L = energy head loss (m)
L = flume length (m)
L_b = floating bridge length (cm)
P_d = pontoon bridge depth (cm)
P_w = pontoon bridge width (cm)
Q = flow discharge (dm^3·s^{-1})
v = mean flow velocity (m·s^{-1})
v_{up} = upstream flow velocity (m·s^{-1})
v_{ds} = downstream flow velocity (m·s^{-1})
y = flow depth (cm)
y_{up} = upstream flow depth (cm)
y_{ds} = downstream flow depth (cm)
ρ = water density of the flow (kg·m^{-3})
μ = dynamic viscosity of water (kg·m^{-1}·s^{-1})

REFERENCES

ABOZAID M.A., ELBEBLAWY M.S.A., SAYED-AHMED E.Y. 2016. Structural performance of hybrid composite pontoon compared to steel. In: Proceedings of 11th International Conference on Civil and Architecture Engineering ICCAE-11-2016. Cairo, Egypt. Military Technical College Kobry GGGEl-Kobbah p. 1–13.

ARNESON L.A., ZEVENBERGEN L.W., LAGASSE P.F., CLOPPER P.E. 2012. Evaluating scour at bridges. Publication No. FHWA-HIF-12-003-HEC18. 5th ed. Hydraulic Engineering Circular No. 18. Washington, DC. U.S. Department of Transportation Federal Highway Administration.

BREDE H. 2017. Concept study and analysis of a floating bridge [online]. MSc Thesis. Trondheim. Norwegian University of Science and Technology pp. 113. [Access 10.08.2020]. Available at: https://ntnuopen.ntnu.no/ntnu-xmlui/handle/11250/2456604?locale-attribute=en

DENG S., FU S., MOAN T., WEI W., GAO Z. 2018. Hydro-elastic analysis of a floating bridge in waves considering the effect of the hydrodynamic coupling and the shore sides. ASME 37th International Conference on Ocean, Offshore and Arctic Engineering. 17–22.06.2018 Madrid, Spain. Vol. 1. Offshore Technology. DOI 10.1115/OMAE2018-78738.

ETTEMA R., NAKATO T., MUSTE M. 2006. An illustrated guide for monitoring and protecting bridge waterways against scour. ProjectTR-515. Final Report. Ames, Iowa. Iowa Highway Research Board, pp. 184.

FREDRIKSEN A.G., HEIERVANG M.F., LARSEN P.N., SANDNES P.G., SØRBY B., BONNEMAIRE B., NESTEBY A., NEDREB Ø. 2019. Hydrodynamical aspects of pontoon optimization for a side-anchored floating bridge. Journal of Offshore Mechanics and Arctic Engineering. Vol. 141(3) p. 1–9. DOI 10.1115/OMAE2017-62698.

HELAL E., SOBEIH M., EZZ EL-DIN M. 2018. Effect of floating bridges on open channels' flow and bed morphology. Journal of Irrigation and Drainage Engineering. Vol. 44(9). DOI 10.1061/(ASCE)IR.1943-4774.0001331.

KOU Y., XIAO L., TAO L., PENG T. 2019. Performance characteristics of a conceptual ring-shaped spar-type VLFS with double-layered perforated-wall breakwater. Applied Ocean Research. Vol. 86 p. 28–39. DOI 10.1016/j.apor.2019.02.011.

MA K., ZHONG J., FENG R., YUAN W. 2019. Investigation of ground-motion spatial variability effects on component and system vulnerability of a floating cable-stayed bridge. Advances in Structural Engineering. Vol. 22(8) p. 1923–1937. DOI 10.1177/1369433219827238.

NEWMAN J.N. 1977. Marine hydrodynamics. Cambridge, USA. The MIT Press. ISBN 9780262140263 pp. 432.

PETERSEN Ø.W., ØISETH O., LOURENS E. 2019. Full-scale identification of the wave forces exerted on a floating bridge using inverse methods and directional wave spectrum estimation. Mechanical Systems and Signal Processing. Vol. 120 p. 708–726. DOI 10.1016/j.ymssp.2018.10.040.

SEIF M., INOUE Y. 1998. Dynamic analysis of floating bridges. Marine Structures. Vol. 11(1–2) p. 29–46. DOI 10.1016/S0951-8339(97)00012-9.

SHIXIAO F., WEICHENG C., XUJUN C., CONG W. 2005. Hydroelastic analysis of a nonlinearly connected floating bridge subjected to moving loads. Marine Structures. Vol. 18 (1) p. 85–107. DOI 10.1016/j.marstruc.2005.05.001.

TOM N.M., MADHI F., YEUNG R.W. 2017. Power-to-load balancing for heaving asymmetric wave-energy converters with noni deal power take-off. Renewable Energy. Vol. 131 p. 1208–1225. DOI 10.1016/j.renene.2017.11.065.

VAN JOHNSON D. 2018. Numerical and experimental investigation of ribbon floating bridges [online]. Master of Applied Science in Civil Engineering, Carleton University, Ottawa, Ontario. [Access 10.08.2020]. Available at: https://curve.carleton.ca/system/files/etd/7cf7f2f5-d91d-431b-a808-f1c69c31f4c8/etd_pdf/034e91f8a88966f7c37966bc7c76511c/van-johnson-numericalandexperimentalinvestigationofribbon.pdf

WANG J., LI L., BOGUNOVIĆ JAKOBSEN J., HAVER S.K. 2019. Metocean conditions in a Norwegian fjord in relation to the floating bridge design. Journal of Offshore Mechanics and Arctic Engineering. Vol. 141(2) p. 1–9. DOI 10.1115/1.4041534.

WEHAUSEN J.V., LAITONE E.V. 1960. Surface waves. In: Encyclopedia of Physics. Vol. 9. Berlin. Springer Verl. p. 446–814.